Journal of Sensor Science and Technology
Vol. 33, No. 6 (2024) pp. 439-447
http://dx.doi.org/10.46670/JSST.2024.33.6.439
pISSN 1225-5475/eISSN 2093-7563

High-Temperature Stable NO_x Sensor for Exhaust Gas Monitoring in Automobiles

Tae Won Ha[1,2,*], Dae-Yun Lim[1,*], and Chil-Hyoung Lee[1,+]

Abstract

Ceramic solid-state electrolytic sensors using electrochemical methods are the most suitable for manufacturing NO_x sensors that can operate reliably over a long period of time in high temperature and corrosive environment of exhaust gases. Unlike other oxides, nitrogen compounds are covalently bonded, and there is no separate conductor for nitrogen ions; therefore, it is not possible to produce sensors based on simple electromotive force measurements. Hence, electrochemical Type III electromotive force measurement, amperometric type, electrical resistance type using oxide semiconductors, and mixed potential-type sensors can be used to measure NO_x. However, Type III electromotive force measurement method is limited in that the melting point of the auxiliary electrode for NO_x detection is lower than the exhaust gas temperature at which the sensor must be driven. The amperometric sensor is not feasible because the electrical signal obtained from the sensor is too weak to discriminate it from other signals, and the oxide electrode is subject to degradation. Therefore, this research aims to develop a solid electrolyte and sensing electrode material that can obtain a high detection signal for NO_x gas even at temperatures above 800°C using a highly sensitive mixed potential method that solves these problems, and develop an algorithm and automotive NO_x sensor that can stably detect NO and NO_2 gas concentrations simultaneously.

Keywords: NO_x sensor, Mixed-potential sensor, Electrochemical detection, Ceramic solid electrolyte, Automotive exhaust gas sensing

1. INTRODUCTION

The automotive NO_x sensor market is expected to reach US $120 billion by 2021 with a growth rate of more than 10%, and is expected to grow to US $160 billion by 2022. The domestic market for automotive NO_x sensors is expected to reach more than 380 billion won by 2023 because diesel cars, which emit harmful gases, have become the main market for automotive denitrification ($DeNO_x$) systems [1,2]. Therefore, it is necessary to develop $DeNO_x$ systems to improve fuel efficiency and reduce NO_x emissions in accordance with the European Union's automotive NO_x emission regulations, and it is crucial to develop high-temperature NO_x sensors that can directly measure NO_x in real time for efficient operation. Most nitrogen oxides (NO_x) are produced when nitrogen and oxygen in air react under high heat during combustion [3]. NO_x is lethal to humans on its own, and it also reacts with various hydrocarbons in the atmosphere to form ozone via a photochemical reaction with sunlight. Despite its usefulness in several industrial applications, ozone contributes to photochemical smog, which significantly reduces air quality [4]. Ozone irritates the mucous membranes of the eyes, causing watery eyes, chest tightness, and development and aggravation of respiratory diseases such as asthma and bronchitis [5]. It is also a strong oxidizing agent that damages plants and their inherent properties, resulting in reduced crop yields. Ozone also oxidizes NO_x and SO_2 in the atmosphere to produce nitric and sulfuric acids, which contribute to acid rain. To reduce NO_x emissions, the emission regulations have been gradually tightened, and strict emission allowance standards have been established to curb emissions from motor vehicles [6]. The emissions that are mainly harmful to human health owing to the increase in number of vehicles in metropolitan areas are unburned hydrocarbons (C_mH_n, 500–1500 ppm), carbon monoxide (CO, 0.5–2.0%), and nitrogen oxides (NO_x, 0.01–0.2%), and ozone (O_3) gas due to the photochemical reactions of NO_x gas in the atmosphere. The health and safety of workers exposed to hazardous gases at industrial sites is of great concern. Therefore, the immediate challenge for

[1]Energy & Nano Technology Group, Korea Institute of Industrial Technology (KITECH)
Gwangju 61012, Republic of Korea
[2]School of Materials Science & Engineering, Chonnam National University
Gwangju 61186, Republic of Korea
*These authors are contrubuted equally to this work.
[+]Corresponding author: chlee0901@kitech.re.kr
(Received: Oct. 31, 2024, Revised: Nov. 5, 2024, Accepted: Nov. 7, 2024)

human health and safety from these combustion gases is to quickly detect and respond to exposure to hazardous gases. In such systems, the application of highly sensitive and reliable NO_x sensors enables miniaturization, portability, mobility, and low-cost NO_x measurement instruments [8,9]. However, the development of NO_x sensors for high-temperature automotive emissions is currently mostly at the NGK level in Japan [10]. In Korea, certain companies such as Iljin and Sejong Corporation and KAIST are developing them; however, their success has not yet been confirmed [11]. There have been several reports published on NO_x measurement at low temperatures (<300°C) using WO_3 semiconductor oxide [12,13]. In the case of automobiles, the temperature of the exhaust gas is high (>800°C), and NO_x sensors that can be used for this purpose have not been developed in Korea. Therefore, it is essential to develop NO_x sensors with features such as miniaturization, high sensitivity, fast response, and selectivity to save energy by improving fuel efficiency and preventing environmental pollution.

2. EXPERIMENTAL METHOD

The manufacturing process of the sensor elements for the development of automotive nitrogen oxide (NO_x) sensors is shown in Fig. 1.

2.1 Ceramic Raw Material Powder

In the tape-casting ceramic molding method, fine powdered ceramic raw materials with a particle diameter of 3 μm or less are used. When manufacturing ceramic sheets using the blade molding method, the composition of the raw material powder, particle size, and distribution of the particle size are significantly influenced by the ultimate sensor element; therefore, it is necessary to consider the characteristics of the starting material to manufacture sheets with excellent sinterability. In this experiment, commercially available YSZ powder (Inframat Advances Materials, LLC 99.95+% / Tosoh, 99.9+%) was used to prepare a green sheet for the solid electrolyte, a mixture of YSZ powder was used as the solid electrolyte, and cordierite ($2Al_2O_3$-$2MgO$-$5SiO_2$) powder of less than 9 wt% was used to prepare a green sheet for the porous diffusion barrier.

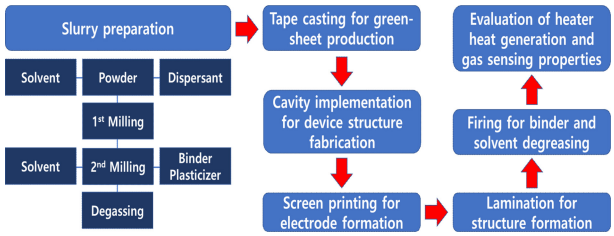

Fig. 1. Manufacturing process of NO_x sensor element

2.2 Selection of Starting Organic Additives

To produce sheets by tape-casting ceramic powders, proper additives must be mixed in appropriate quantities. These additives, which are mainly organic, impart strength and plasticity to the ceramic sheet, ensure uniform dispersion of the ceramic powder in the solvent, and significantly affect the properties of the ceramic sheet during casting. Therefore, knowledge is acquired through repeated experiments. Although the selection of organic additives is an important experimental process, a broad selection criterion has not yet been established; hence, proper organic additives were selected through experiments for basic research.

2.3 Slurry Preparation and Tape Casting

Because the simultaneous addition of dispersants, plasticizers, and binders makes it difficult for organic matter to be competitively adsorbed onto the surface of the particles, thereby preventing complete dispersion, a homogeneous slurry was prepared by first mixing the solvent, dispersant, and YSZ powder with zirconia balls, followed by a second mixing with binders and plasticizers. In this experiment, MEK+Ethanol was used as a solvent, PEG was used as a dispersant and binder to maintain the strength of the sheet, and DBP was used as a plasticizer to loosen the bonds and impart plasticity to the sheet to prepare a slurry for tape casting. As the bubbles generated by the vapor pressure of air and solvent entering the slurry cause defects in the sheet, the slurry was subjected to a defoaming process by stirring at a constant speed under reduced pressure to remove the bubbles and excess solvent added for mixing, and to obtain a viscosity suitable for molding tape castings. The defoamed slurry was tape-cast and molded using a doctor blade. The tape carrier film was a polyethylene film with a thickness of 100 μm and a width of 170 mm, coated with SiO_2 on the surface. The tape transport speed was 30 cm/min and blade height was 1.65 mm for the first and 1.15 mm for the second.

2.4 Processing of Green Sheet

2.4.1 Cutting

The prepared green sheets were cut to fit the size of the sensor

elements. In this experiment, the green sheet for the solid electrolyte was first cut to a size of 7 mm × 80 mm, and then the two cavity layers in the device were cut to the appropriate size. The cutting machine was an STC-10B (Hansung Systems, Inc.).

2.4.2 Screen Printing

An experiment was conducted to print patterns, such as heaters, reference electrodes, and sensing electrodes, on a green sheet after cutting. The panel used for printing was divided into different materials to minimize the loss of paste during printing, as shown in Fig. 4. In addition, in the case of green sheets printed on both sides, drying was performed in an oven at 50°C for 10 min after printing on one side to prevent damage to the pattern.

2.4.3 Lamination

After printing, lamination was performed to integrate the green sheets. Lamination was performed by varying pressure, temperature, and holding time based on the structural diagram of the manufactured sensor element. Depending on the condition of the green sheet, the temperature was 40–120°C, the pressure was 10–150 kgf/cm^2, and the holding time was 1–60 min to ensure that the sensor element was not deformed.

2.4.4 Co-firing

The NO_x sensor elements fabricated through lamination were subjected to heat treatment. The most important part of the heat treatment step is to degrease the amount of various organic solvents used during the green sheet manufacturing and establish conditions that can prevent cracking, bending, and warping of the device during heat treatment. For this purpose, the removal temperature of the organic solvent and shrinkage temperature of the green sheet were determined prior to heat treatment. In addition, the damage caused by the direct heat applied to the sample during heat treatment was prevented.

3. RESULTS AND DISCUSSIONS

3.1 Green Sheet of Ion Conducting Layer and Diffusion Barrier Layer

The two types of green sheets used in this study are solid electrolyte layer for ionic conduction and diffusion barrier layer. Because complete solubility could not be obtained when using a single solvent alone, good solubility results were obtained using mixed solvents. In addition, plasticizers were used appropriately

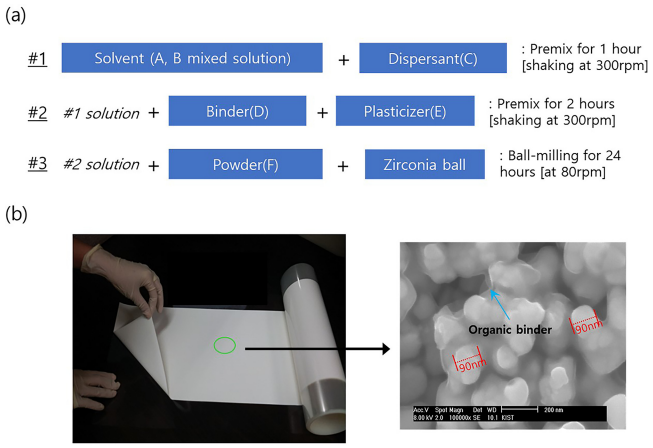

Fig. 2. (a) Schematic of green sheet fabrication method, and (b) fabricated green sheet sample and SEM image

to control viscosity and suppress adhesion to the film. The plasticizers contained in the green sheet decompose during heat treatment to prevent cracking of the green sheet owing to interaction with each other when it burned [14,15]. A 30 cm × 100 cm pilot green sheet without cracks was manufactured by adjusting the type and amount of the binder and organic solvent. Fig. 2 (a) shows the mixing sequence and proportions of the solvent, binder, dispersant, and plasticizer used to prepare the green sheet. Fig. 2 (b) shows a sample of the prepared green sheet and its structure obtained using SEM analysis.

3.2 Detector Electrode Manufacturing

3.2.1 Preparation of Sensing Powder

$ZnFe_2O_4$ and $ZnCr_2O_4$ were selected as sensing materials. Using ZnO (Aldrich Chemical Co, Ltd 99.9%), Fe_2O_3 (Aldrich Chemical Co. Ltd., 99.9%), and Cr_2O_3 (Aldrich Chemical Co. Ltd., 99.9%) as starting materials, Zn:Fe or Zn:Cr in a molar ratio of 1:2 was mixed using a wet ball mill for 24 h and then heat treated at 1600°C for 4 h to obtain synthesized $ZnFe_2O_4$ and $ZnCr_2O_4$. Fig. 3 (a) shows the XRD patterns of the synthesized $ZnFe_2O_4$ and $ZnCr_2O_4$ powders [16]. All synthesized powders exhibited single-phase spinel crystal structures.

3.2.2 Preparation of Sensing Electrode Paste

The sensing electrode powders were mixed with the solvents and binders listed in Table 1, and prepared as a paste in a three-roll mill. The paste thus prepared was applied to alumina by screen printing method and dried at 50°C for 30 min [17,18]. The dried paste was heat treated at 1600°C to form a sensing electrode

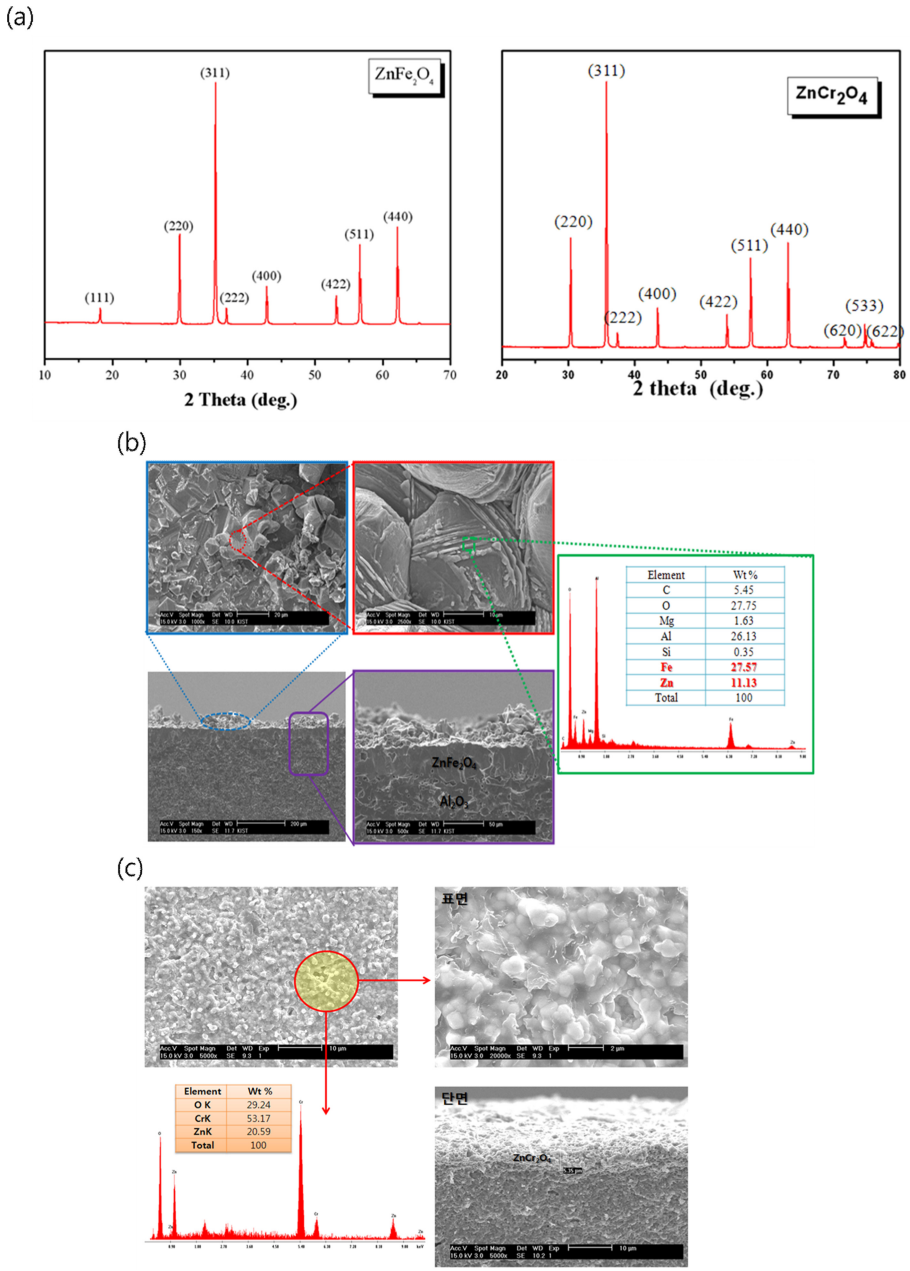

Fig. 3. (a) XRD patterns of synthesized $ZnFe_2O_4$ and $ZnCr_2O_4$ powders, (b) SEM microstructure and composition of $ZnFe_2O_4$ sensing electrode, and (c) SEM microstructure and composition of $ZnCr_2O_4$ sensing electrode

Table 1. Sensing electrode paste preparation (Mixing ratio of solvent, binder, and additives)

Sensing electrode paste		
	$ZnFe_2O_4$ / $ZnCr_2O_4$ powder	40 wt%
Solvent	Toluene	40 wt%
Binder	PMMA	10 wt%
Additives	α-terpineol, BCA(Butyl Carbitol Acetate)	10 wt%

and analyzed by SEM and EDS to confirm its printability and composition (Figs. 3 (b) and 3 (c)).

3.3 NO_x Sensor Structure Design and Fabrication

The NO_x sensor device for automotive use was designed to improve the oxygen pumping efficiency and detection of NO and NO_2 using a diffusion barrier layer, as shown in Fig. 4 (a) [19,20]. The designed NO_x sensor is a next-generation NO_x sensor with improved sensitivity achieved by controlling the oxidation-reduction rate of NO and NO_2 on the oxide sensing electrode to improve the detection of NO and NO_2 by improving the oxygen

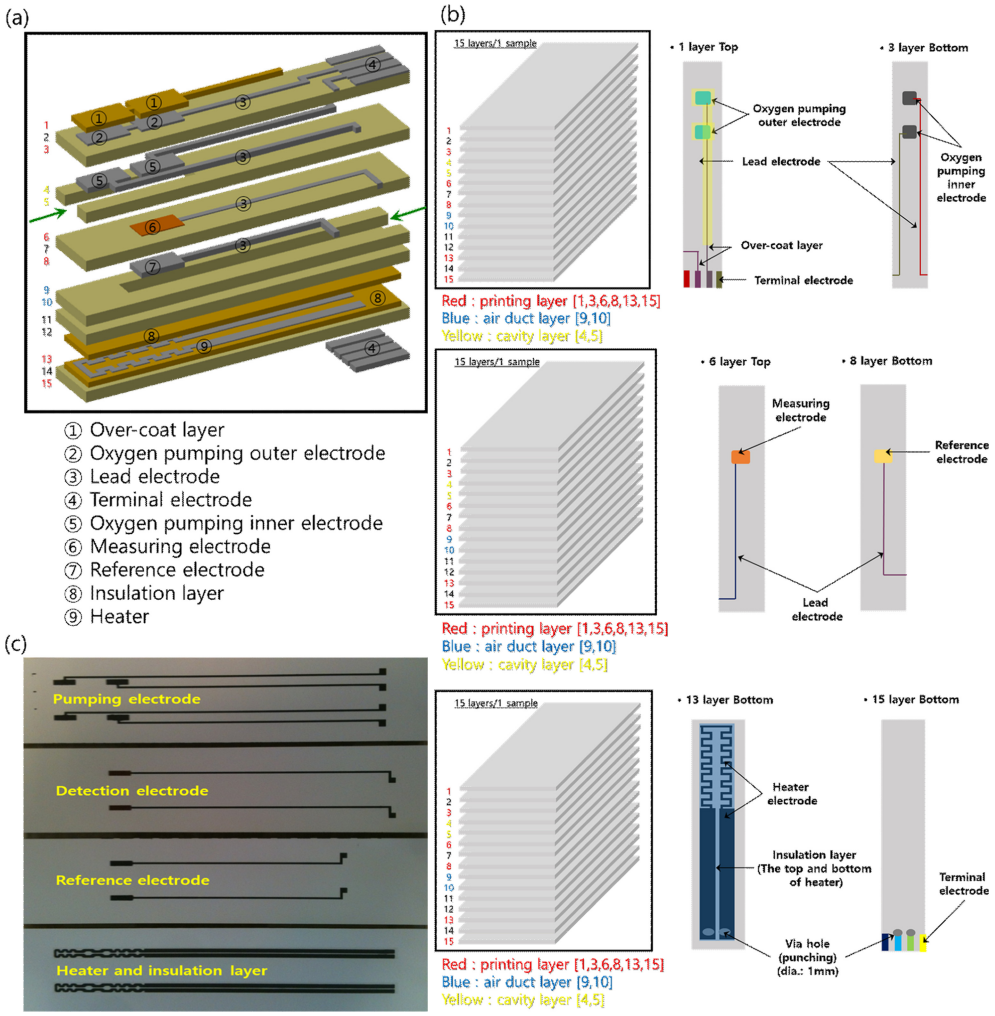

Fig. 4. (a) Structural schematic of the proposed NO_x sensor, (b) Detailed schematic of each layer of the sensor element, and (c) Images of the formation of electrodes and insulation layers used in the sensor element

pumping efficiency and using a diffusion barrier layer, as shown in Fig. 4 (a) [21]. The nitrogen oxide sensor was designed using 15 green sheets. Each layer has a complex structure, as shown in Fig. 4 (b). The top surface of the first layer consists of an external oxygen-pumping electrode, a terminal electrode, and a lead electrode, which are protected by a porous protective layer and an insulating layer. An internal oxygen-pumping electrode and lead electrode were formed underneath the third layer, and the exhaust gas cavity was separated into two parts. The sixth and eighth layers formed the detection and reference electrodes, respectively, and the air duct was the bottom layer. In the third layer, a heater is formed between the insulating layers. The bottom of the fifth layer is composed of terminal electrodes, including heater terminals, which must be precisely controlled during mass production. In addition, to reduce the defect rate of the sensor element, the process was optimized to prevent adhesion between the paste and the green sheet, and short circuit of each pattern. When printing the heater pattern embedded in the sensor element, insulation layers of 15–30 μm thickness were formed above and below the heater to prevent the deterioration of the heater due to the applied voltage and to block the leakage current from the detection cell or pumping cell. In addition, an insulating layer and a porous protective layer were simultaneously formed to protect the electrode and lead electrode responsible for oxygen pumping outside the sensor, and the sensor element was manufactured to significantly improve the sensing characteristics (Fig. 4 (c)).

3.4 Analysis of the Structure and Composition of the Sensor Element After Heat Treatment

After the heat-treated NO_x sensor specimens were cut using a cutting machine, the solid electrolytic zirconia sheet, internal and

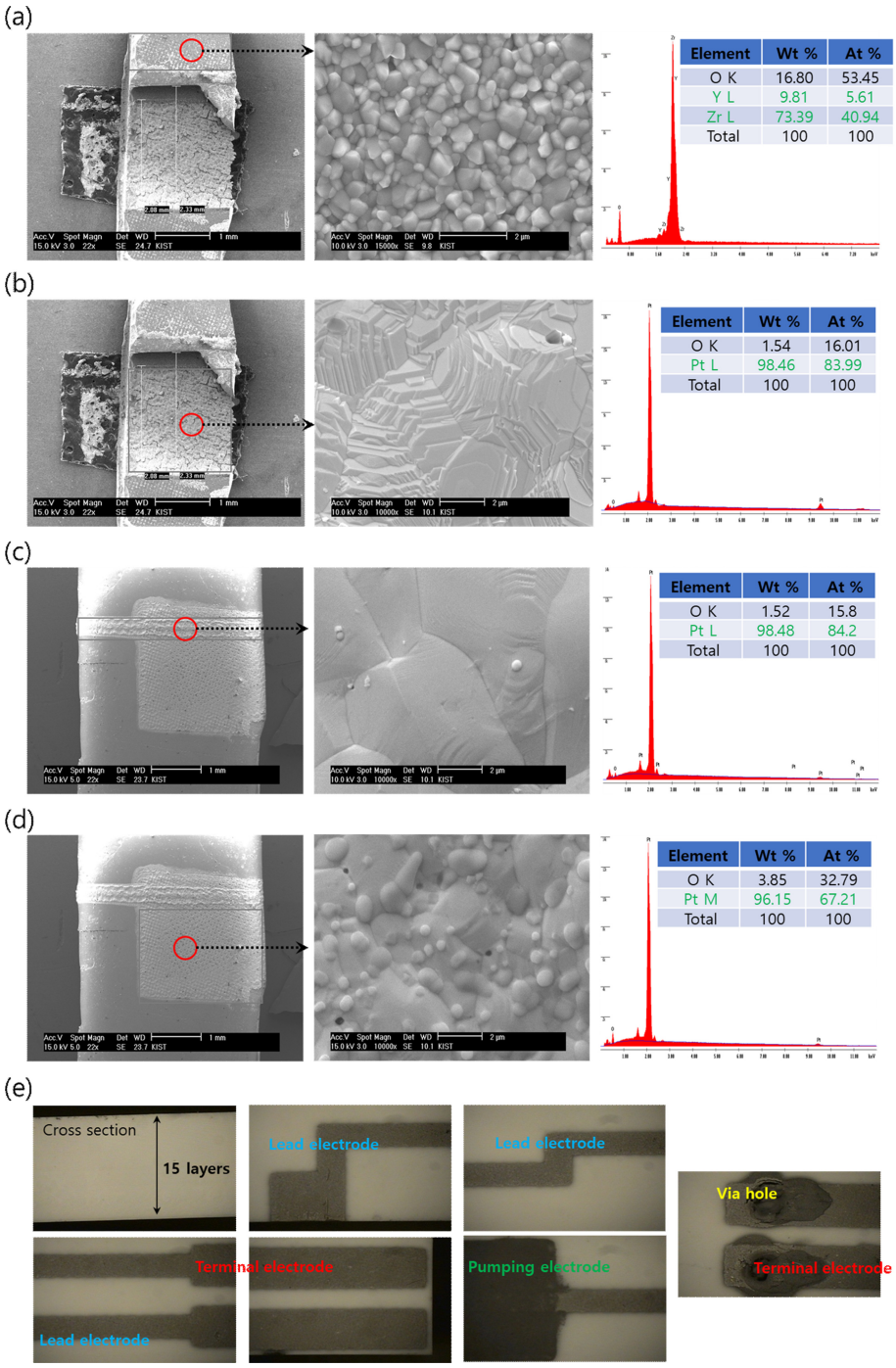

Fig. 5. Microstructure and composition analysis images of (a) solid electrolytic zirconia sheet, (b) internally pumped Pt electrode, (c) externally pumped lead electrode, (d) externally pumped Pt electrode, and (e) optical microscopy image of the external shape of the sensor after firing

external pumped Pt electrodes, and external lead electrodes were analyzed using an electron microscope (Figs. 5 (a-c)), and the external morphology of the NO_x sensor after firing was observed using an optical microscope (Fig. 5 (d)). The results showed that the interior of the green sheet had a fairly good filling of organic additives and ceramic powder, with few cracks and residual organic matter. This indicates that the selection of the organic additives according to the ceramic powder is appropriate, and that the conditions of the green sheet are satisfied in that it is possible to form an electrode of a certain thickness in the green sheet state and that no burn-out, bending, or cracking occurs during the manufacture of the sensor element. In addition, the reference,

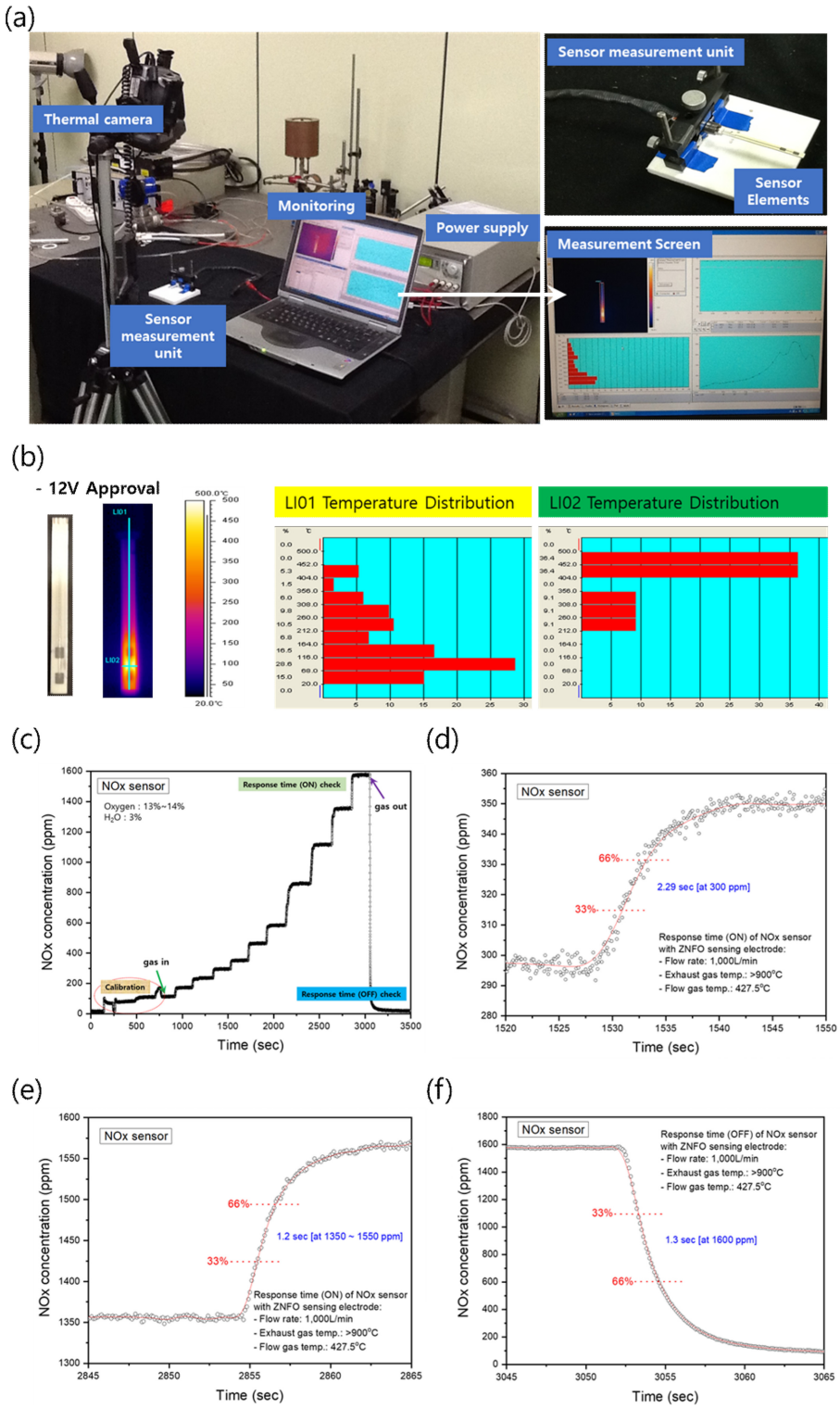

Fig. 6. (a) Infrared thermal imaging camera measurement of sensor element, (b) heater heating test result of NO_x sensor, (c) analysis of sensing signal according to NO_x concentration change, (d) response characteristics of NO_x sensor (ON, at NO_x 300 ppm), (e) response characteristics of NO_x sensor (ON, at NO_x 1350–1500 ppm), and (f) response characteristics of NO_x sensor (OFF, at NO_x 0 ppm)

pumping, and detection electrodes showed little volatilization or diffusion of the electrode, even after heat treatment.

A test of the heater integrated into the nitrogen oxide sensor element was performed using an infrared thermal imaging camera. The temperature distribution of the entire sensor element and the temperature distribution of the heating area, where the oxygen-

pumping, detection and reference electrodes were located, were investigated while maintaining 12 V. Fig. 6 (a) shows the infrared thermal imaging camera measurements, and Fig. 6 (b) shows the thermal test results of the fabricated nitrogen oxide sensor. Nitrogen oxide sensors directly measure the combustion gases in automotive exhaust, and hence, they should be able to operate at high temperatures of 700–800°C. As shown in Fig. 6 (b), the heater in the device is maintained at a temperature >800°C, which is sufficient for high temperature operation. Fig. 6 (c) shows the sensing signal as the NO_x concentration changed under the conditions of 13–14% oxygen and 3% moisture. The results showed that a wide range of NO_x concentrations can be detected and that the sensing signal changed stably with gas in/out. The time required for a sensor to detect a certain concentration of a test gas is called the response time; the faster the response time, the better the sensor. Figs. 6 (d-f) shows the response characteristics of the nitrogen oxide sensor at gas temperatures above 800°C as a function of time. The response time of the sensor obtained in this study was ON (at NO_x 300 ppm): 2.29 s, ON (at NO_x 1350–1500 ppm): 1.2 s, OFF (at NO_x 0 ppm): 1.3 s, which is higher than that of the world's best sensor (NGK, 0.75 s); this is a very good result compared to the response time of most of the solid electrolyte sensors studied previously, which was more than 3 s.

4. CONCLUSIONS

In this study, an automotive NO_x sensor was developed by fabricating a solid electrolyte green sheet with ion conducting and diffusion barrier layers, which served as the foundation for producing the sensor component and assessing its high-temperature NO and NO_2 sensing performance. The automotive NO_x sensor structure was designed using a mixed-potential mechanism, which enables regulation of NO and NO_2 redox reactions, while incorporating an internal heater, porous protective layers, and an insulation to prevent degradation and leakage current. The post-sintering analysis confirmed that electrode diffusion and cracking were effectively minimized, resulting in a uniform structure. Infrared thermography further verified that the heater maintained stable heat distribution at temperatures exceeding 800°C. In addition, NO_x response characteristics were evaluated at gas temperatures above 800°C, and the sensor demonstrated a response time of 1.2–2.29 s, showing significant improvement in speed and stability compared to conventional solid electrolyte sensors. These results indicated that the developed NO_x sensor could reliably detect NO_x with high accuracy and speed under high-temperature conditions, indicating its practical applicability in automotive exhaust gas monitoring.

ACKNOWLEDGMENT

This research was supported by a grant of the Korea Evaluation Institute of Industrial Technology (KEIT) funded by the Korean government (MOTIE) (RS-2023-00257663), (RS-2023-00235283) and the Korea Institute of Industrial Technology (KITECH, Project no. UR240004).

REFERENCES

[1] G. Coppola, V. Pugliese, and S. Chakraborty, *"De-NO_x SCR, catalysts and process designs in the automotive industry," in Advanced technologies for solid, liquid, and gas waste treatment*, Y.-C. Ho, W. J. Lau, S. Chakraborty, N. Rajamohan, and S. A. Arni, Eds. CRC Press, Boca Raton, 2023.

[2] I. Nova and E. Tronconi, *Urea-SCR technology for DeNO_x after treatment of diesel exhausts*, *Part of the book series: Fundamental and applied catalysis (FACA)*, New York, Springer, NY, pp. 1-716, 2014.

[3] S. C. Hill and L. Douglas Smoot, "Modeling of nitrogen oxides formation and destruction in combustion systems", *Prog. Energy Combust. Sci.*, Vol. 26, No. 4-6, pp. 417-458, 2000.

[4] S. Madronich, M. Shao, S. R. Wilson, K. R. Solomon, J. D. Longstreth, and X. Y. Tang, "Changes in air quality and tropospheric composition due to depletion of stratospheric ozone and interactions with changing climate: implications for human and environmental health", *Photochem. Photobiol. Sci.*, Vol. 14, pp. 149-169, 2015.

[5] I. S. Mudway and F. J. Kelly, "Ozone and the lung: a sensitive issue", *Mol. Aspects Med.*, Vol. 21, No. 1-2, pp. 1-48, 2000.

[6] N. Hooftman, M. Messagie, J. V. Mierlo, and T. Coosemans, "A review of the european passenger car regulations – Real driving emissions vs local air quality", *Renewable Sustainable Energy Rev.*, Vol. 86, pp. 1-21, 2018.

[7] Q. Li, W. Zeng, and Y. Li, "Metal oxide gas sensors for detecting NO_2 in industrial exhaust gas: Recent developments", *Sens. Actuators B Chem.*, Vol. 359, p. 131579, 2022.

[8] P. K. Sekhar, Z. Moore, S. Aravamudhan, and A. Khosla, "A new low-temperature electrochemical hydrocarbon and NO_x sensor", *Sensors*, Vol. 17, p. 2759, 2017.

[9] M. C. Alvareza, S. F. Puertoa, P. Arroyo, C. M. Rodríguez, and E. P. Gil, "A portable, low-cost, smartphone assisted methodology for on-site measurement of NO_2 levels in ambient air by selective chemical reactivity and digital image analysis", *Sens. Actuators B Chem.*, Vol. 338, p.

129867, 2021.

[10] O. L. Figueroa, C. Lee, S. A. Akbar, N. F. Szabo, J. A. Trimboli, P. K. Dutta, N. Sawaki, A. A. Soliman, and H. Verweij, "Temperature-controlled CO, CO_2 and NO_x sensing in a diesel engine exhaust stream", *Sens. Actuators B Chem.*, Vol. 107, No. 2, pp. 839-848, 2005.

[11] J. Park, B. Y. Yoon, C. O. Park, W.-J. Lee, and C. B. Lee, "Sensing behavior and mechanism of mixed potential NO_x sensors using NiO, NiO(+YSZ) and CuO oxide electrodes", *Sens. Actuators B Chem.*, Vol. 135, No. 2, pp. 516-523, 2009.

[12] T. S. Kim, Y. B. Kim, K. S. Yoo, G. S. Sung, and H. J. Jung, "Sensing characteristics of dc reactive sputtered WO_3 thin films as a NO_x gas sensor", *Sens. Actuators B Chem.*, Vol. 62, No. 2, pp. 102-108, 2000.

[13] M. Penza, C. Martucci, and G. Cassano, "NO_x gas sensing characteristics of WO_3 thin films activated by noble metals (Pd, Pt, Au) layers", *Sens. Actuators B Chem.*, Vol. 50, pp. 52-59, 1998.

[14] Y.-J. Oh and C.-H. Lee, "Limit-current type zirconia oxygen sensor with porous diffusion layer", *J. Sens. Sci. Technol.*, Vol. 17, No. 5, pp. 329-337, 2008.

[15] T. Liu, X. Wang, L. Li, and J. Yu, "Review: Electrochemical NO_x gas sensors based on stabilized zirconia", *J. Electrochem. Soc.*, Vol. 164, No. 13, pp. B610-B619, 2017.

[16] S. Zhuiykov, T. Ono, N. Yamazoe, and N. Miura, "High-temperature NO_x sensors using zirconia solid electrolyte and zinc-family oxide sensing electrode", *Solid State Ionics*, Vol. 152-153, pp. 801-807, 2002.

[17] R. Faddoul, N. R. Bruas, and A. Blayo, "Formulation and screen printing of water based conductive flake silver pastes onto green ceramic tapes for electronic applications", *Mater. Sci. Eng. B*, Vol. 177, No. 13, pp. 1053-1066, 2012.

[18] M. V. Nikolic, Z. Z. Vasiljevic, M. D. Lukovic, V. P. Pavlovic, J. B. Krstic, J. Vujancevic, N. Tadic, B. Vlahovic, and V. B. Pavlovic, "Investigation of $ZnFe_2O_4$ spinel ferrite nanocrystalline screen-printed thick films for application in humidity sensing", *Int. J. Appl. Ceram. Technol.*, Vol. 16, No. 3, pp. 981-993, 2019.

[19] F. H. Garzon, R. Mukundan, and E. L. Brosha, "Solid-state mixed potential gas sensors: theory, experiments and challenges", *Solid State Ionics*, Vol. 136-137, pp. 633-638, 2000.

[20] T. Ritter, J. Zosel, and U. Guth, "Solid electrolyte gas sensors based on mixed potential principle: A review", *Sens. Actuators B Chem.*, Vol. 382, p. 133508, 2023.

[21] F. A. Ali, D. K. Mishra, R. Nayak, and B. Nanda, "Solid-state gas sensors: sensing mechanisms and materials", *Bull. Mater. Sci.*, Vol. 45, p. 15, 2022.